Carbon Stocks in Peri-Urban Areas: A Case Study of Remote Sensing Capabilities

Paolo Villa, Francesco Malucelli, and Riccardo Scalenghe

***Abstract*—Peri-urban areas are the extension of cities into contiguous areas, where households and farms coexist. Carbon stocks (CSs) assessment, a concept here extended to urban features, has not yet been studied in depth over peri-urban areas due to uncertainties in such CSs quantification, level of detail required about construction materials, and the high spatial variability of those stocks. Remote sensing (RS)-based techniques have been successfully utilized in urban areas for assessing phenomena such as soil sealing, sprawl patterns, and dynamics of surface imperviousness, especially focusing on land cover classification at high to medium spatial scales. Over the floodplain study area of Emilia-Romagna region (Italy), we compared mapping products derived from Landsat multiseasonal data with different CSs, in soils and impervious surfaces, such as buildings and roads. A multiscale correlation analysis and regression assessment between CSs layers and satellite products were run at different grid cell sizes (100, 250, 500, and 1000 m). Results show that RS products from processing of mid-resolution satellite data can effectively perform well enough to estimate CSs in peri-urban areas, especially at 500–1000 m scale. Urban Fraction Cover method, derived through weighting urban land cover classes (including dense, sparse, and industrial urban features) can represent a good proxy of the ratio of anthropogenic over natural CSs (R^2 up to 0.75). Imperviousness Index (II) product scored high positive correlation with CSs over built-up areas (R^2 up to 0.77), and strong negative correlation with organic carbon density in soil (R^2 up to 0.73).**

***Index Terms*—Carbon stocks (CSs), remote sensing (RS), Landsat, peri-urban area.**

I. Introduction

UNDER a business-as-usual scenario, the projected global temperature increase might be in the order of 2–6 °C by 2100 [1] as consequence of imbalanced carbon stocks (CSs). The Kyoto Protocol, dealing with such CSs changes, has raised the need to forecast a global terrestrial biosphere budget. But this global budget depends on different land use types and their individual carbon (C) densities, determined both by land use and environmental factors [2], [3]. Cost-effective reduction of greenhouse gases net emissions into the atmosphere, and relative CSs accounting, is quite a difficult task to tackle. A change in C density within a specified area is credited or debited to the responsible stakeholder, and then computed at national level [4]. Measuring the change in average CSs, annual credits/debits must be divided by a time constant but they must be measured, above all. They are usually measured by collecting samples and analyzing them in laboratory. In natural and seminatural areas, the estimation of CSs is currently reliable [5], [6]; however, in peri-urban environments, a certified procedure does not exist yet.

A peri-urban mixed space, or peri-urban area, is an extension of metropolitan areas into a contiguous rural areas where households and farms coexist [7]–[9]; here, CSs in the soil, as below-ground pattern, are intensely influenced by human activities [10]–[12], as well as the above-ground CSs, including forests clearance [13]. We must point out that even if the term "carbon stocks" usually is applied to rural and natural areas only, the concept is broader; in particular, here we are extending the use of the term to urban features as well. The characteristic of these areas is their temporal dynamics: a soil covered by forests and natural areas, or cultivated land can transform into urban settlements very quickly (some years). Usually, the dynamics patterns start in the form of isolated changes within the area, and then agglomerations tend to congregate into larger nuclei, creating urban sprawl. On these issues, a massive literature exists that does not need to be mentioned in detail here, just to avoid unjustified preferences.

With rare exceptions, the soil CSs are usually mapped by masking out or assigning a zero value to urbanized areas; see e.g., [14]. This means that the balance of CSs is done on the basis of nonurbanized areas mainly. But what if the urbanized area extension in some regions is not negligible, compared with rural/natural land cover? Peri-urban areas become preponderant and their contribution to CSs budget as well. In addition to this fact, these areas are changing very quickly over time.

Studies on urbanization have revealed that anthropogenic activities affect CSs on land surface [15], especially near the peri-urban limits or urban fringes; nevertheless, their role has not been comprehensively considered yet, even if it has been demonstrated to be quite important [16]–[18]. This is because it is difficult to map themselves and their changes. But these areas contain C, and this carbon is currently cut off from maps. Mapping urban areas using remote sensing (RS) data has been widely studied but most of the applications dealing with anthropic CSs are focusing on dense urban environment and small areal coverage [19]. Manual surveying techniques are usually used for small areas but if their sizes increase, semiautomatic approaches are to be preferred because of their cost-effectiveness [19], as these practices require investments and time. For this reason, it is not possible to obtain maps of the

Manuscript received October 25, 2013; revised April 23, 2014; accepted May 20, 2014.

P. Villa is with the Institute for Electromagnetic Sensing of the Environment, National Research Council (IREA-CNR), 20133 Milan, Italy (e-mail: villa.p@irea.cnr.it).

F. Malucelli is with the Servizio Geologico, Sismico e dei Suoli, 40127 Bologna, Italy.

R. Scalenghe is with the Dipartimento Scienze Agrarie e Forestali (SAF), Università degli Studi di Palermo, 90133 Palermo, Italy.

Color versions of one or more of the figures in this paper are available online at http://ieeexplore.ieee.org.

Digital Object Identifier 10.1109/JSTARS.2014.2328862

stocks with short time intervals using traditional methods. A reliable estimate of CSs in peri-urban areas has not yet been studied extensively due to the uncertainties in their quantification at local level, requiring detailed knowledge of construction materials and abundances, and the high spatial variability and heterogeneity of those stocks [20].

RS and imaging spectroscopy have demonstrated their usefulness in studying CSs in forest and soil land cover areas [21], [22]. A number of works have been published during the last two decades, covering the topic of estimation of soil organic carbon (SOC) content using multispectral data [23]–[25]. Moreover, RS-based techniques have been successfully utilized for assessing urban area phenomena such as soil sealing, sprawl patterns and dynamics, and surface imperviousness, especially through land cover classification at high to medium spatial scale [26], [27]. A preliminary analysis of RS capabilities in providing information about anthropogenic C in urban and peri-urban areas has been recently run by Villa *et al.* [28], which found good correlation patterns over the Emilia-Romagna (ER) region, in northern Italy, between reference "anthropogenic carbon-organic carbon" ratio values and both imperviousness and urban features cover derived from RS data (R^2 0.6–0.7). Conversely, this work aims to compare different RS urban features maps derived from Landsat data with reference CSs datasets, covering SOC, C in built-up land, and "anthropogenic carbon-organic carbon" ratio.

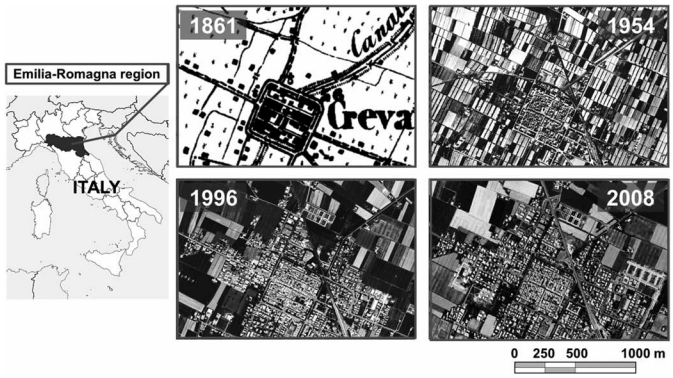

Fig. 1. Snapshot of urban area evolution in ER region, during the last 150 years, focusing on the small town of Crevalcore ($44\ ^{\circ}43'$N $11\ ^{\circ}09'$E, 133 inhabitants km^{-2} in 2010). The ratio between natural+rural land use and urban+industrial land use was 17 in 1861, dropped to 9 in 1954, 3 in 1976, and 2 in 1996. Since 2008, the two land uses occupy, more or less, equal surface areas.

II. Study Area and Dataset

A. Study Area Overview

We have selected the ER region as the study area for our work. The reason is that there exists a mapping of the CSs of the floodplain that sum also urban stocks. ER is a highly anthropized area, hosting massive economic activities. ER is of the size of Jamaica but it is located in Italy on the right bank of the Po River. It occupies a great part of the main Italian floodplain and it is inhabited by three million people. Around one tenth of Italian gross domestic product comes from ER, including a significant share of the national arable production and animal farming activities. Natural and anthropogenic CSs in ER region have undergone considerable modifications during the last century, under the huge influence of anthropic activities [29]: an increase of anthropogenic fraction of CSs from less than 1% in the middle of the 19th century to almost 10% today occurred. This result originates from major changes that occurred to land use, and in particular, the reduction in extensive animal farming, the nearly complete disappearance of orchards/intercropping, replaced by intensive production agriculture, and soil sealing due to urbanization (Fig. 1). The natural and cultivated areas are currently in the same order of magnitude of the urbanized space in numerous areas of ER.

B. CSs Dataset

The C dataset used as reference in this work comes from the work of Scalenghe *et al.* [26], in which CSs in the ER floodplain were studied, identifying CSs contribution from the soil (organic material and carbonates), from plants (trees, orchards, and vineyards), and from impervious surfaces (concrete from buildings and infrastructures, and asphalt in roads and parking lots). Moreover, they delivered a functional index map of the study area, describing soil sealing degree in form of ratio between anthropogenic (C in concrete and asphalt) over natural (SOC and C in trees) CSs (named: [Cc]/[Co]), which relied on land cover information coming from existing thematic cartography. For each of the above-mentioned CSs layers and for the [Cc]/[Co] index, Scalenghe *et al.* [29] built a raster GIS layer with a cell size of 100 m, which is used in this work as reference CSs data to be compared with RS-derived products.

Three layers of CSs were used here, all of them referring to the 2003 year situation: organic carbon density in soils (identified here as Co_soil), the carbon density in built-up surfaces, concrete and asphalt (C_built-up), both of them measured in $\mathrm{Mg\ ha}^{-1}$ of C, and the [Cc]/[Co] index (Cc-Co), a unitless ratio. Soil CSs data refer to the first 30 cm of the soil. The maps were built using soil data routinely collected and analyzed between 1981 and 2005, with most of the data presented here collected between 1988 and 1999 [30]. The entire database contains 18 969 geo-referenced sites on approximately $12\,000\ \mathrm{km}^2$. The CS layer related to the trees was built using the Corine Land Cover codes relative to wood, orchards, and vineyards with specific values of C densities [29], [31]. The below-ground biomass CS has been taken into account only in the "bulk" stock of the tree, where epigean and hypogean stocks were together accounted for [29]. The concrete CSs layer was built using data from the regional land cover map [31] and from census data. A map of C density was derived by reconstructing volumes and the relative C content per area, and analogously the CS in asphalt were estimated using the maps of the roads where a value of C density was measured for each specific type of local road [29].

C. Satellite Dataset

The RS dataset is composed of eight Landsat TM/ETM+, acquired in different seasons and covering the temporal range from summer 2001 to summer 2003. The spatial coverage of the entire study area is spanning over two WRS-2 tiles, one for the west part and one for the east part of ER region (path 192-row 29;

path 193-row 29, respectively). The eight Landsat scenes were grouped into four seasonal composites, which are listed as follows, according to the identifying code "Landsat sensor"_ "scene date West part (WRS-2 tile: path-row)"–"scene date East part (WRS-2 tile: path-row)":

1) Summer 2001 composite: ETM+_26 August 2001 (192-29)—01 August 2001 (193-29);
2) Spring 2002 composite: TM_17 May 2002 (192-29)—01 June 2002 (193-29);
3) Winter 2002-03 composite: ETM+_21 February 2002 (192-29)—13 March 2003 (193-29);
4) Summer 2003 composite: TM_24 August 2003 (192-29) —16 September 2003 (193-29).

The satellite scenes in the dataset were subject to preprocessing, including radiometric calibration for top of atmosphere reflectance retrieval, based on calibration coefficients provided by USGS together with Landsat data ancillary information, and first-order atmospheric effect correction for retrieval of ground reflectance values, according to the Dark Object Subtraction (DOS) approach [32], [33], using low albedo surfaces (i.e., deep and clear water pixels) as reference dark objects. Finally, couple of scenes from homologous season have been mosaicked for deriving the four seasonal composites listed above.

III. Methods

A. Methodological Approach Introduction

The methodological approach adopted in this work is based on exploiting spectral indexes coming from normalized difference spectral band ratios [27], to derive information about imperviousness and urban land cover features from mid-resolution satellite data. Such approach has been already tested and successfully applied to real case studies in previous works [27], [34], [35]. The spectral indexes used for such purpose are as follows.

NDVI—Normalized Difference Vegetation Index: A vegetation index based on spectral characteristics of green vegetation in the visible red and near-infrared ranges (TM-ETM+ bands 3 and 4, respectively) [36]; NDVI multitemporal features can be exploited to distinguish vegetated surfaces by other land cover classes, and its intra-annual variability can help in differentiating agricultural, managed areas from natural vegetation; NDVI formula used here is (where ρ is ground reflectance)

$$\mathbf{NDVI} = \frac{\rho_{\mathrm{NIR}}(TM/ETM{+}_{band\,4}) - \rho_{\mathrm{RED}}(TM/ETM{+}_{band\,3})}{\rho_{\mathrm{NIR}}(TM/ETM{+}_{band\,4}) + \rho_{\mathrm{RED}}(TM/ETM{+}_{band\,3})}. \quad (1)$$

SVI—Soil and Vegetation Index: A perviousness index based on visible short wavelengths and shortwave infrared response (TM-ETM+ bands 1 and 5, respectively), for distinguishing nonimpervious (soil and vegetation, mainly) from highly impervious surfaces and water [27], [34]; SVI multitemporal features can be exploited to separate water-related cover features (water bodies, wetlands, and paddy rice fields) from other land cover classes, and can be used for distinguishing highly impervious industrial features from barren land cover surfaces; SVI formula used here is (where ρ is ground reflectance)

$$\mathbf{SVI} = \frac{\rho_{\mathrm{SWIR1}}(TM/ETM{+}_{band5}) - \rho_{\mathrm{BLUE}}(TM/ETM{+}_{band1})}{\rho_{\mathrm{SWIR1}}(TM/ETM{+}_{band5}) + \rho_{\mathrm{BLUE}}(TM/ETM{+}_{band1})}. \quad (2)$$

UI—Urban Index: An index of artificial surface cover, based on the spectral response of urban features in near-infrared and shortwave infrared ranges (TM-ETM+ bands 4 and 7, respectively) [37]; UI multitemporal features can be exploited to map urban cover features, in densely and sparsely urbanized areas, distinguishing these features from agricultural- and vegetation-related land cover; UI formula used here is (where ρ is ground reflectance)

$$\mathbf{UI} = 1 + \frac{\rho_{\mathrm{SWIR2}}(TM/ETM{+}_{band7}) - \rho_{\mathrm{NIR}}(TM/ETM{+}_{band4})}{\rho_{\mathrm{SWIR2}}(TM/ETM{+}_{band7}) + \rho_{\mathrm{NIR}}(TM/ETM{+}_{band4})}. \quad (3)$$

Starting from these indexes, three different RS urban features products were derived, for each of the four seasonal 2002–2003 Landsat composites, in form of: 1) thematic mapping of anthropic surfaces density resulting from dense and residential urban cover features derived for land cover classification, Urban Fraction Cover_method 1 (UFC_1) product; 2) thematic mapping of anthropic surfaces density resulting from dense, residential, and industrial urban cover features derived for land cover classification, Urban Fraction Cover_method 2 (UFC_2) product; and 3) mapping of impervious surfaces intensity, Imperviousness Index (II) product. UFC_1 and UFC_2 derivation process and their definition are described in Section III-A1.

For UFC_1 and UFC_2 derivation, a land cover map focused on urban surfaces cover (Land Cover 2002–2003 map) was produced starting from multiseasonal NDVI, SVI, and UI index features. II derivation was based on processing of multitemporal series of UI only. Such products, exemplified in Fig. 2, for the sample area of Modena urban district within ER region and their derivation are described in Section III-B1–B3.

1) Land Cover Mapping: Land cover mapping, to be used for finally deriving UFC_1 and UFC_2 products, has been performed starting from multitemporal statistics coming out of the four seasonal Landsat composites for 2002–2003. From the multispectral reflectance scenes, three normalized index (SVI, NDVI, and UI) maps were derived for each of the four seasonal composites (Summer 2001, Spring 2002, Winter 2002–2003, and Summer 2003). The average multiseasonal values (SVI_mean, NDVI_mean, and UI_mean) and multiseasonal standard deviation values (SVI_std, NDVI_std, and UI_std) were derived. These six multiseasonal feature layers were used as input for a general 2002–2003 land cover classification schema for ER region, aimed at mapping 10 land cover classes: 1) Urban_dense; 2) Urban_mixed; 3) Urban_industrial; 4) Vegetation_permanent; 5) Agricultural_vegetated; 6) Agricultural_soil; 7) Barren land; 8) Water; 9) Wet

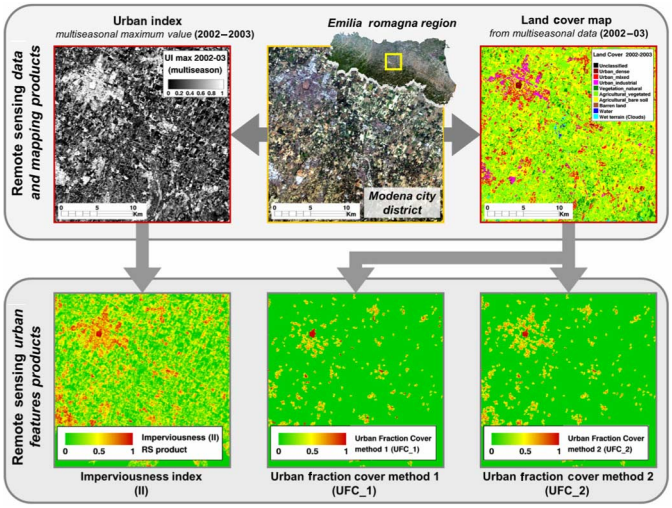

Fig. 2. RS products derived from Landsat TM-ETM+ data and spectral indexes, in the area of Modena city district, central ER region. Top panel shows satellite data and intermediate mapping products, from left to right: UI mapping for 2002–2003, true color Landsat data (summer 2002 composite), land cover map for 2002–2003. Bottom panel shows urban feature products, described in the text: II, UFC_1, and UFC_2 (from left to right).

terrain; and 10) Clouds. The classification approach has been originally developed in previous works, [28] and [33], and is based on a supervised binary decision tree. Decision thresholds were set for each node in the tree based on multiseasonal statistics derived of input features, collected over selected reference areas for which the land cover is well known; then, those separation thresholds were used for designing a pixel-based, binary cascade decision tree classifier. This work uses the same decision tree schema and thresholds already used in [28], for the ER floodplain. An example of classification algorithm can be described using the "Urban_dense" class as a reference. A pixel is detected as "Urban_dense" cover class, for the temporal range 2002–2003, when it shows low variability of spectral index responses across different seasons ($\mathrm{SVI\_std} < 0.2$ and $\mathrm{NDVI\_std} < 0.175$), together with null to little vegetation cover features ($\mathrm{NDVI\_mean} < 0.2$), and when the mean multiseasonal urban index value is very low ($\mathrm{UI\_mean} < 0.0$). According to these rules, the decision tree classification implemented in [28] finally leads to labeling a pixel as class "Urban_dense." Land cover classification accuracy was assessed over a subset of ER region corresponding to Bologna province area ($3700\ \mathrm{km}^2$, roughly 16.5% of ER region area), using thematic cartography of land cover as reference. For allowing a correct thematic matching of classified and reference data, land cover classes were grouped into four groups: 1) urban; 2) natural vegetation; 3) crop land; and 4) barren land. The land cover classification produced scored an overall accuracy of 86.6%, and a Kappa coefficient of 0.775, while urban land cover class true positive rate is of 84.1%.

B. RS Urban Features Products

Land cover map of 2002–2003 and multitemporal values of UI based on Landsat scenes were used as intermediate products for finally deriving RS products of urban and peri-urban areas features to be compared with reference CSs density layers. Such final RS urban features maps are derived as multiscale products, at four spatial scales (grid cell side: 100, 250, 500, and 1000 m), resampling Landsat original resolution (30 m); they are named UFC_1, UFC_2, and II, and details about their derivation are provided as follows.

1) Urban Fraction Cover—Method 1 (UFC_1): UFC_1 product, which aims to express urban cover intensity, excluding industrial features, was derived through a simple weighting procedure of two urban cover classes in the land cover map for 2002–2003: for this, "Urban_dense" class, representing dense residential areas and city centers, has been given unitary weight, while "Urban_mixed" class, representing residential areas of sparse urbanization with mixed pervious and impervious surfaces, has been given 0.5 weight. Eventually, UFC_1 product for the year 2002–2003 comes from the weighted average of those two land cover classes.

2) Urban Fraction Cover—Method 2 (UFC_2): UFC_2 product, aiming to express urban cover intensity by also including industrial features, was derived through a simple weighting procedure of all the three urban cover classes in the land cover map for 2002–2003. "Urban_dense" class has been given unitary weight, while both "Urban_mixed" and "Urban_industrial" classes have been give 0.5 weight. Eventually, UFC_2 product for the year 2002–2003 comes from the weighted average of those three land cover classes.

3) Imperviousness Index: II product was derived from UI multiseasonal layers, because they were assessed as more effectively representing the imperviousness features of urban and peri-urban areas in ER region. A maximization approach was adopted, for filtering out UI value distortions due to seasonal variability of natural surfaces and minimizing disturbances due to bare terrain surfaces, which can result in UI values similar to some urban features (especially in sparsely urbanized areas); this consisted of selecting, for each pixel in the scenes, only the highest value of UI scored over the four multiseasonal composites used. Therefore, II product for the year 2002–2003 comes from the mapping of maximum UI scores over the four seasons represented in the dataset.

This study originates from the work of Villa *et al.* [28] results and implements them by investigating correlations between various CSs layers and urban features. For such purposes, the three urban features products derived according to the described methodological approach (UFC_1, UFC_2, and II) were tested against three reference CSs products (Co_soil, C_built-up, and Cc-Co).

IV. Results and Discussion

Once the urban features products described were derived from RS data covering 2002–2003 temporal range, the resulting maps (UFC_1, UFC_2, and II) were compared with the reference layers of CSs and densities features, derived by Scalenghe *et al.* [29] for 2003, in terms of organic carbon density in soil (Co_soil), CSs density in built-up surfaces (C_built-up), [Cc]/[Co] ratio (Cc-Co), at resampling scales of 100, 250, 500, and 1000 m.

Fig. 3 shows the representation of the reference CSs maps [3(d)–(f)], as well as the RS products [3(a)–(c)], for a 100 m spatial resampling scale.

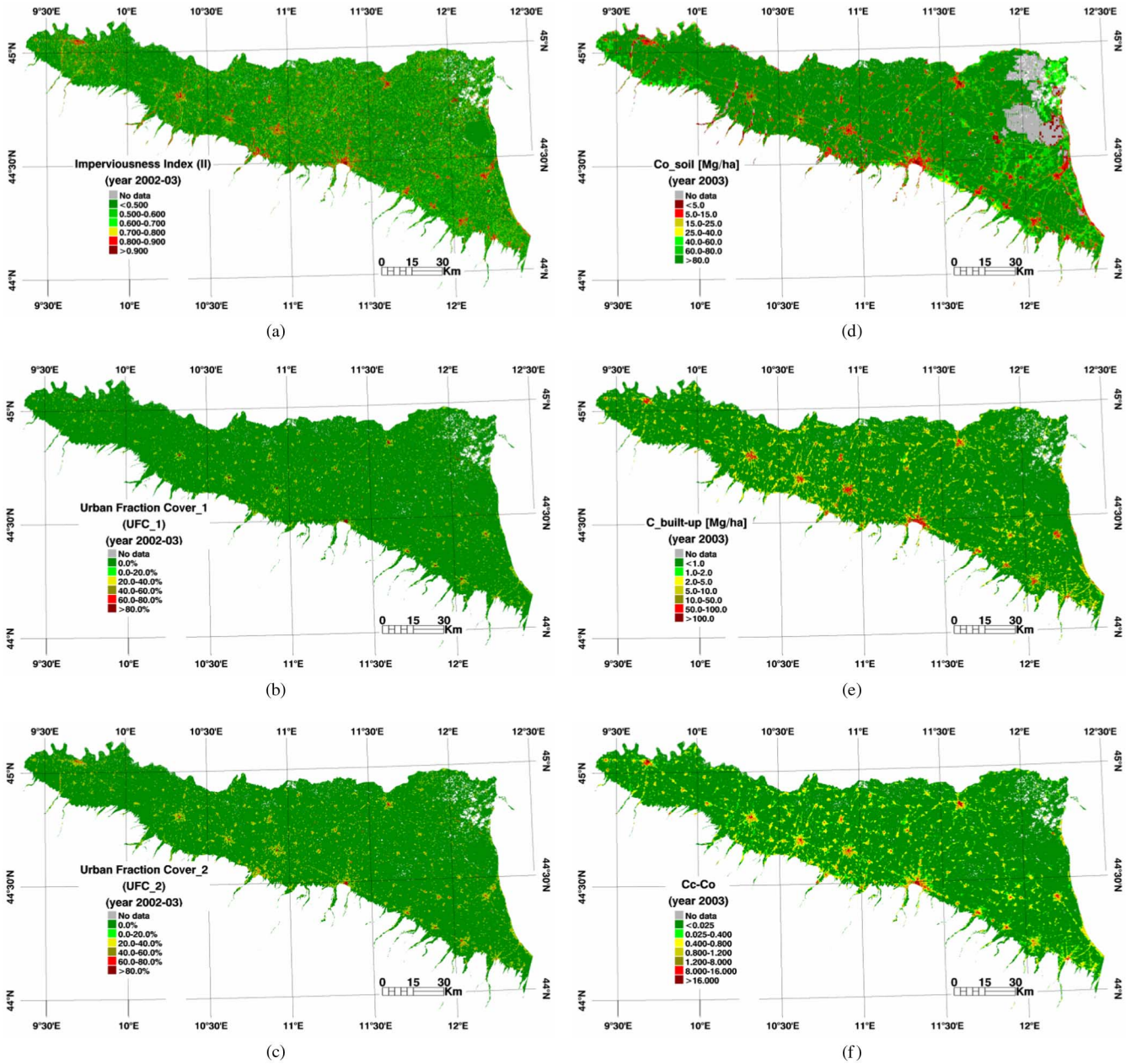

Fig. 3. RS urban features mapping products [left column: (a)–(c)] and reference CSs layers [right column: (d)–(f)] over ER floodplain study area, displayed at 100 m of spatial grid scale: (a) II for year 2002–2003; (b) UFC_1 for year 2002–2003; (c) UFC_2 for year 2002–2003; (d) Co_soil for year 2003 (with inverse graduation color scale with respect to other panels); (e) C_built-up for year 2003; and (f) Cc-Co for year 2003. White spots in North-East of the study area are due to masking of cloud covered areas in Landsat scenes, and correspond to rural land cover regions.

Notes:
II: Imperviousness Index calculated using multitemporal satellite data, for year 2002–2003;
UFC_1: Urban Fraction Cover calculated from land cover classification, by using method 1 (Industrial land cover features excluded) for year 2002–2003;
UFC_2: Urban Fraction Cover calculated from land cover classification, by using method 2 (Industrial land cover features included) for year 2002–2003;
Co_soil: reference of organic carbon density in soils for year 2003, calculated according to [26];
C_built-up: - reference CSs layer of carbon density in built-up surfaces for year 2003, calculated according to [26];
Cc–Co: reference layer of anthropic-organic carbon ratio ([Cc]/[Co] ratio) for year 2003, calculated according to [26];
Log: logarithmic regression model;
R^2: coefficient of determination for regression models (linear or logarithmic);

Spatial scale of observation is a key issue to be considered in environmental and landscape analyses, particularly, in urban and peri-urban areas which are inherently characterized by high level of heterogeneity in their surface features and materials composition. Concentrated around the rural-urban duality, different information on peri-urban areas can be extrapolated depending on the spatial scale at which the urbanization phenomena and dynamics are analyzed [38]. Here, our aim is to assess the feasibility of estimating CSs of anthropogenic origins in urban fringes through RS.

Therefore, the assessment of results coming out of this work has been run in form of multiscale analysis, in particular,

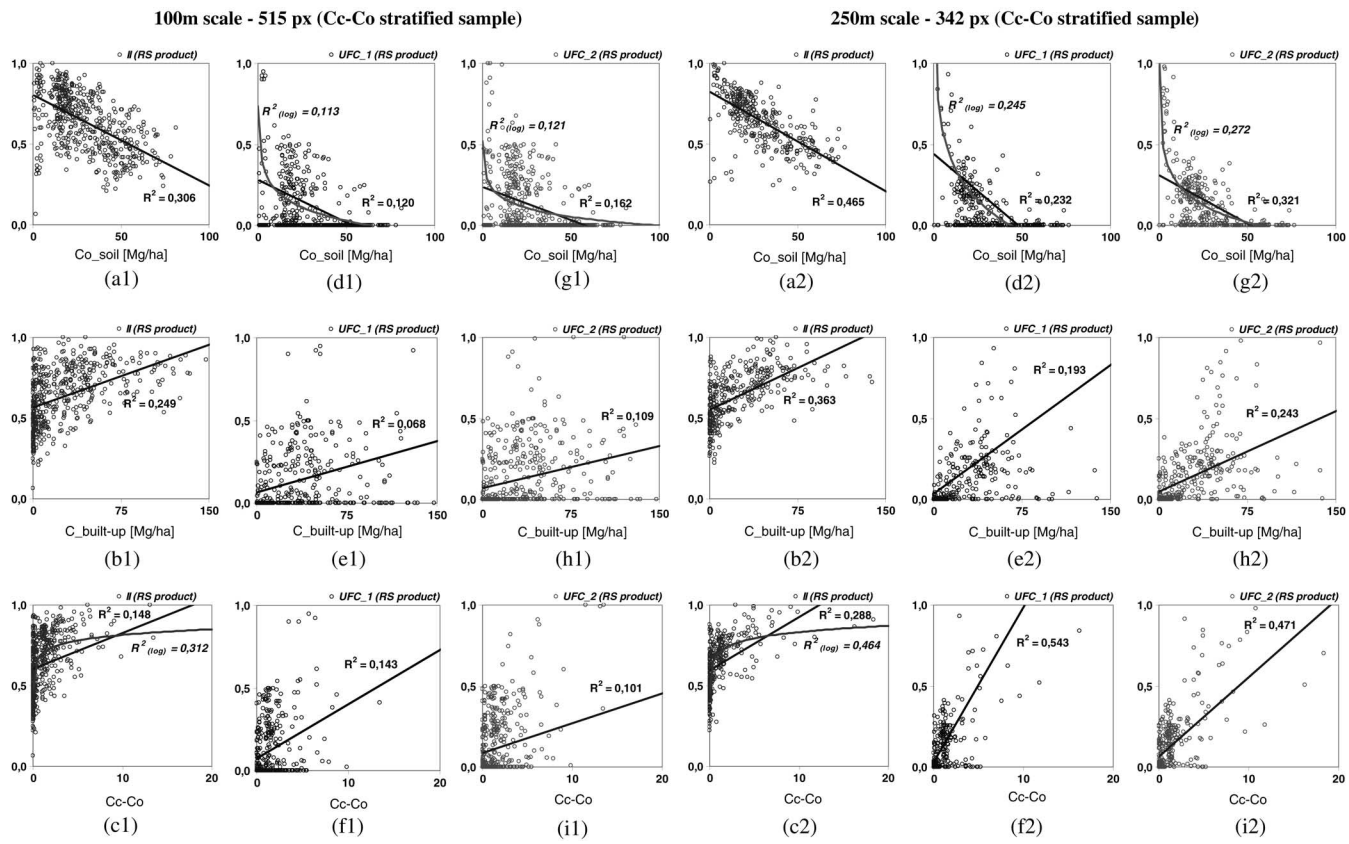

Fig. 4. Scatter plots and correlation scores for RS-derived products and reference CSs layers for year 2003, calculated using stratified random sampling at 100 m spatial scale [panel (a1)–(i1), on the left] and 250 m spatial scale [panel (a2)–(i2), on the right]: (a1–a2) II versus Co_soil; (b1–b2) II versus C_built-up; (c1–c2) II versus Cc-Co; (d1–d2) UFC_1 versus Co_soil; (e1–e2) UFC_1 versus C_built-up; (f1–f2) UFC_1 versus Cc-Co; (g1–g2) UFC_2 versus Co_soil; (h1–h2) UFC_2 versus C_built-up; (i1–i2) UFC_2 versus Cc-Co.

differentiating four scales according to spatial grid density at which RS urban features and CSs layers are resampled and compared: 100 (minimum spatial scale coinciding with reference CSs layers grid resolution), 250, 500, and 1000 m cell side.

Correlations between each of the RS urban features maps derived for the year 2002–2003 (UFC_1, UFC_2, and II) have been calculated in comparison with the CSs features layers of year 2003 (Co_soil, C_built-up, Cc-Co) coming from [29], over random samples extracted at four scales (100, 250, 500, and 1000 m). Samples were extracted following an approach based on random sampling stratified over the range of values of Cc-Co (range covered: 0–20): 515 samples were extracted for 100 m scale, 342 samples were extracted for 250 m scale, 195 samples were extracted for 500 m scale, and 143 samples were extracted for 1000 m scale.

Scatter plots of RS urban features products against CSs layers are shown in Fig. 4 (100 and 250 m scales) and Fig. 5 (500 and 1000 m scales), together with coefficients of determination (R^2) of each variable regression.

The variability of R^2 with spatial scale and CSs layer regression against RS urban features products are compared in Fig. 6. Each regression coefficient of determination has been tested for significance and every one passed p-value test (F function) with 0.0001 cutoff probability, so that each of the regression correlations calculated can be considered statistically highly significant.

CSs layers and remotely sensed urban features are related. This is what emerges from the quantitative analysis of results shown in scatter plots of Figs. 4 and 5 and from variations in R^2 with spatial scale (Fig. 6). These results are highlighting specific trends that link CSs layers and different remotely sensed urban features, which are described in the next paragraphs.

UFC_1 and UFC_2 products show generally low to medium correlation with Co_soil and C_built-up ($\mathrm{R}^2 < 0.55$), but good correlations with Cc-Co ($\mathrm{R}^2 > 0.68$) [Fig. 6(b) and (c)]. Correlation trends for UFC_1 and UFC_2 show marked linearity and positive correlation with Cc-Co values [Figs. 4(f)–(i) and 5(f)–(i)], which are less disperse for low Cc-Co. UFC_2 outperforms UFC_1 when compared to Co_soil and C_built-up [Fig. 6(b) and (c)], but even more when compared to Cc-Co ($\mathrm{R}^2 = 0.74$), particularly at low resolution scale (1000 m). Correlation of UFC_2 with C_built-up stocks values is lower than with Cc-Co, but still notable, peaking $\mathrm{R}^2 = 0.55$ at 1000 m scale.

II product shows matching with Co_soil and C_built-up stocks [Fig. 6(a)] which is better than with UFC_1 and UFC_2, at every spatial scale. In particular, II shows very good linear inverse agreement with increasing Co_soil values ($\mathrm{R}^2 = 0.62$ at 500 m scale, $\mathrm{R}^2 = 0.77$ at 1000 m scale), in Figs. 4(a) and 5(a), and with C_built-up ($\mathrm{R}^2 = 0.73$ at 1000 m scale), in Figs. 4(b) and 5(b), this one with positive correlation. II product behavior against Cc-Co, instead, is characterized by sensible saturation for higher Cc-Co values [Figs. 4(c) and 5(c)], so that logarithmic regression is

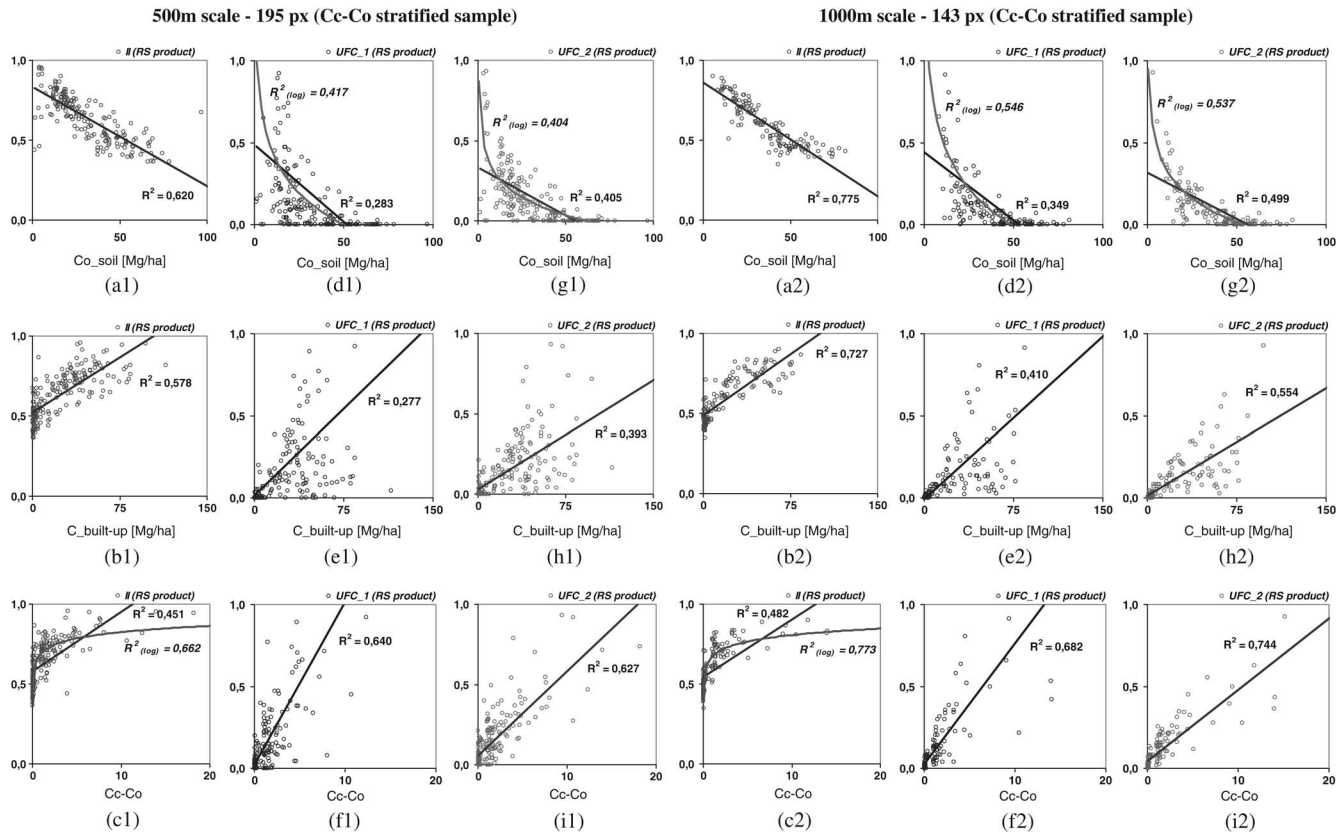

Fig. 5. Scatter plots and correlation scores for RS-derived products and reference CSs layers for year 2003, calculated using stratified random sampling at 500 m spatial scale [panel (a1)–(i1), on the left] and 1000 m spatial scale [panel (a2)–(i2), on the right]: (a1–a2) II versus Co_soil; (b1–b2) II versus C_built-up; (c1–c2) II versus Cc-Co; (d1–d2) UFC_1 versus Co_soil; (e1–e2) UFC_1 versus C_built-up; (f1–f2) UFC_1 versus Cc-Co; (g1–g2) UFC_2 versus Co_soil; (h1–h2) UFC_2 versus C_built-up; (i1–i2) UFC_2 versus Cc-Co.

performing better than linear regression at every spatial scale, peaking at $R^2 = 0.66$ at 500 m scale and $R^2 = 0.77$ at 1000 m scale.

Regarding the specific capabilities of RS products in representing different CSs features over ER region, results show that II could be effectively act as both an inverse proxy of Co_soil and a direct proxy of C_built-up, through the establishment of linear regression models (which is a topic out of the scope of this work), while a logarithmic regression model could be set up to estimate Cc-Co from II scores, paying attention to saturation of II for high Cc-Co values. Imperviousness of land cover derived from multispectral data is, therefore, detected here as the most important feature linked with CSs in urban and peri-urban areas. As for urban fraction cover features mapping, UFC_2 product generally outperforms UFC_1; this proves that industrial cover features are playing a nonnegligible role in accounting for CSs of urban areas and could be usefully exploited alone or in integration with II for estimating C_built-up and especially Cc-Co, because of the linearity (nonsaturated) of UFC_2 behavior over a wide range of Cc-Co values, differently to II.

Features such as the dispersion of UFC_2 values and the saturation of II for higher values of Cc-Co indicate that remotely sensed products are more effectively able to act as proxy for this CSs in areas where urbanization is less dense (Cc-Co < 4-5), which are generally corresponding to peri-urban areas and urban fringes. As stated in Section I, such areas are the most sensitive from a urban sprawl point of view, and are the less investigated from the aspect of anthropogenic CSs, because of their heterogeneity and fast dynamics.

The multiscale analysis has assessed that the best correlation results are reached for low resolution spatial scales, 500 and 1000 m. This fact can be linked with some commission error (overestimation) of urban features identification over rural areas, in cases when barren land and bare soil surfaces can result in spectral response similar to that of some type of urban cover. The correlation of higher spatial scale results with reference data would be true if the accuracy of the RS was always 100%, but unfortunately this is not the case for any RS methodology published. For example, land cover products derived from RS are usually judged highly accurate when their thematic error, expressed in overall accuracy, is higher than 90%, but this means that a residual error over up to 10% of the classified area is still present. The relatively scarce availability of good quality and cloud-free Landsat scenes over ER region for the years 2002–2003 (only eight scenes) can also contribute to less than ideally reliable land cover maps classification, reflecting into UFC_1 and UFC_2, whose possible if low error level can affect correlation results when compared with CSs reference layers.

As a preview of possible usefulness of the outcomes coming from our work, we carried out an exercise over seven detail sites of $9\ \mathrm{km}^2$ size, spread around the ER region and featuring a variety of peri-urban characteristics and intensities. For these areas, we calculated CSs in Mg using best linear regression

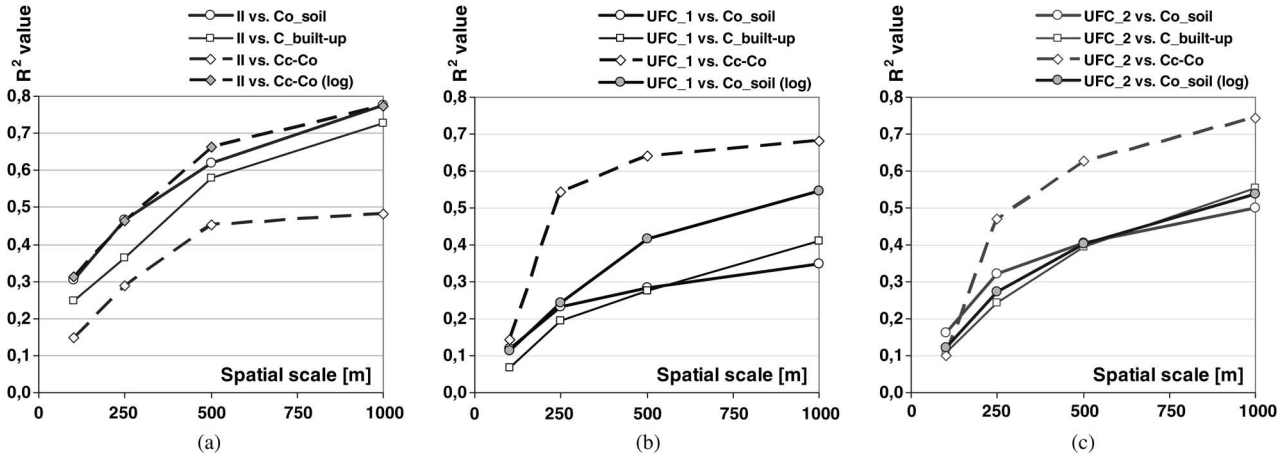

Fig. 6. R^2 variability plotted against four different spatial scales and three distinct CSs layers, for the three RS urban features products tested: (a) II; (b) UFC_1; and (c) UFC_2.

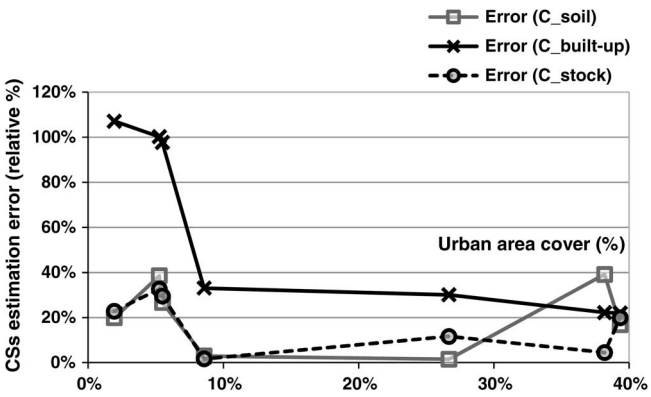

Fig. 7. CSs estimation error calculated with respect to reference CSs data, plotted against urban area percent cover for $9\ \mathrm{km}^2$ experimental sites collected over ER region, in terms of relative estimation value (% error).

coming out of results shown in Fig. 5(a2) and (h2) (Co_soil and C_built-up, and the corresponding total C_stocks), and we compared them with real case CSs calculated using Scalenghe *et al.* [29] method. Some variability of CSs estimation error was found depending on the area, but a clear decreasing trend in error is evident when the areas analyzed are more densely urbanized. In particular, Fig. 7 shows that relative estimation error for C_built-up is very high (100–110%) in very sparsely anthropized areas with less than 10% urban cover spatial percentage, and falls to acceptable levels (around 30% and less) for areas with higher urban fraction, while Co_soil estimation is more stable over the range of urban fraction percent covered (around 20%).

Such figures, even if only a preview calculated over small, detailed areas, support our idea that RS could be used as a tool for estimating CSs with a tolerable degree of error and over wide areas, and particularly for urban and peri-urban areas with sensible urban surface cover ($>15\%$). Our results demonstrate that urban features mapped from RS can play a role in CSs assessment in peri-urban areas when a certain error level in estimation is allowed and especially when *in situ* accurate data are not enough or too costly. In this context, RS could be an added value for urban CSs estimation in terms of: spatializing existing *in situ* high quality and accurate data, multitemporal analysis when *in situ* data are not acquired frequently enough to follow the urban sprawl dynamics, fast and low cost assessment in case of large areas to be covered (regional to continental scale).

V. Conclusion

This methodological approach, based on urban features maps from multiseasonal normalized indexes derived by Landsat data, shows that RS products can effectively perform well enough to estimate CSs especially at 500–1000 m spatial scale. Among products tested, Urban Fraction Cover (UFC_2) is the best proxy of Cc-Co (R^2 up to 0.75), mainly for over peri-urban areas (Cc-Co < 4-5).II demonstrated notable correlation with Co_soil (negative correlation, $R^2 = 0.62 - 0.77$ for 500–100 m scale) and C_built-up (positive correlation, $R^2 = 0.73$ at 1000 m scale), while a saturation effect has been noticed when comparing II to Cc-Co (Cc-Co > 5). Land cover imperviousness is confirmed as a crucial feature even in estimating CSs in peri-urban areas.

Studies on the topic of urban sprawl, or the evolution of peri-urban fringe, generally do not consider the fact that its changes involve substantial interferences with the strategic functions carried out by soil, functions of which carbon is a significant expression. The good correlation between the calculated indexes and CSs could allow for the design of a model for estimating CSs and their changes, based on land use features in peri-urban areas. In particular, our correlations score reached for coarse resolution spatial scales (500–1000 m) suggest the possible use of low resolution satellite dataset (e.g., MODIS) for assessing peri-urban CSs over wider areas. In addition to their wide coverage, such satellite data have the advantage of enhanced temporal resolution (compared to Landsat), maintaining the low cost.

The measurements of CSs are generally carried out in the natural and rural environment, not taking into account the weight of urbanization. The speed with which the amount of carbon varies in these environments is extremely rapid. Estimated costs of errors in standard sampling for carbon accounting span from 0.01 to 8 EUR (11 USD) per tonne of carbon [39], based on the sample size required to achieve sampling error level from 10% to

zero. Extrapolating these hypotheses in our study area, ER region, annual accounting error costs could span from ≈ 300 kEUR (400 kUSD) to 150 million EUR (≈ 210 million USD) in the zero error sampling scenario. The use of a quick and reliable estimation technique, which exploits RS synoptic datasets also in integration with *in situ* and laboratory data, could reduce the total cost of carbon accounting by augmenting the intensity of sampling in time and space. To make a map of CSs, a complex analytical procedure is required. It is made of multitemporal soil surveys, sampling, and chemical analysis in the laboratory. Once validated locally, RS methodologies coupled with techniques of reflectance spectroscopy [40] and [41], might provide (nondestructive) rapid prediction of CSs in the short-term, with acceptable level of error compared to costs.

In summary, our results foresee an application of RS in integrating information to current ongoing studies about anthropogenic CSs in peri-urban areas, even in the context of adding informative layers to spatial regression and interpolation approaches. The comparison of the estimation error with traditional techniques is a necessary condition to suggest the use of RS as an alternative and will be the subject of future works.

References

[1] IPCC, *Climate Change 2007: The Physical Science Basis*. Cambridge U.K.: Cambridge Univ. Press, 2007.

[2] C. S. B. Grimmond, T. S. King, F. D. Cropley, D. J. Nowak, and C. Souch, "Local-scale fluxes of carbon dioxide in urban environments: Methodological challenges and results from Chicago," *Environ. Pollut.*, vol. 116, pp. S243–S254, 2002.

[3] M. A. Imhoff *et al.*, "The consequences of urban land transformation on net primary productivity in the United States," *Remote Sens. Environ.*, vol. 89, pp. 434–443, 2004.

[4] M. U. F. Kirschbaum *et al.*, "A generalised approach of accounting for biospheric carbon stock changes under the Kyoto protocol," *Environ. Sci. Policy*, vol. 4, pp. 73–85, 2001.

[5] G. P. Asner, "Tropical forest carbon assessment: Integrating satellite and airborne mapping approaches," *Environ. Res. Lett.*, vol. 4, 2009, doi: 10.1088/1748-9326/4/3/034009.

[6] G. P. Asner *et al.*, "High-resolution mapping of forest carbon stocks in the Colombian Amazon," *Biogeosciences*, vol. 9, pp. 2683–2696, 2012.

[7] I. Zasada, C. Fertner, A. Piorr, and T. Sick Nielsen, "Peri-urbanisation and multifunctional adaptation of agriculture around Copenhagen," *Danish J. Geogr.*, vol. 111, pp. 59–72, 2011.

[8] R. J. Alig and R. G. Healy, "Urban and build-up land area changes in the U.S.: An empirical investigation of determinants," *Land Econ.*, vol. 63, pp. 215–226, 1987.

[9] J. Cavailhès, D. Peeters, E. Sékeris, and J. F. Thisse, "The periurban city: Why to live between the suburbs and the countryside," *Reg. Sci. Urban Econ.*, vol. 34, pp. 681–703, 2004.

[10] C. Cloquet, J. Carignan, and G. Libourel, "Isotopic composition of Zn and Pb atmospheric depositions in an urban/periurban area of Northeastern France," *Environ. Sci. Technol.*, vol. 40, pp. 6594–6600, 2006.

[11] R. Scalenghe and F. Ajmone-Marsan, "The anthropogenic sealing of soils in urban areas," *Landscape Urban Plann.*, vol. 90, pp. 1–10, 2009.

[12] U. Schleuß, Q. Wu, and H. P. Blume, "Variability of soils in urban and periurban areas in Northern Germany," *Catena*, vol. 33, pp. 255–270, 2009.

[13] K. Krutilla, W. F. Hyde, and D. Barnes, "Periurban deforestation in developing countries," *Forest Ecol. Manage.*, vol. 74, pp. 181–195, 1995.

[14] A. Ruesch and H. K. Gibbs, "New IPCC tier-1 global biomass carbon map for the year 2000," Oak Ridge National Laboratory, Oak Ridge, TN, USA, 2008 [Online]. Available: http://URLcdiac.ornl.gov

[15] L. R. Hutyra, B. Yoon, and M. Alberti, "Terrestrial carbon stocks across a gradient of urbanization: A study of the Seattle, WA region," *Global Change Biol.*, vol. 17, pp. 783–797, 2011.

[16] G. Churkina, "Carbon cycle of urban ecosystems," in *Carbon Sequestration in Urban Ecosystems*, R. Lal and B. Augustin, Eds. New York, NY, USA: Springer, 2012, pp. 315–330.

[17] R. V. Pouyat, I. D. Yesilonis, and N. E. Golubiewski, "A comparison of soil organic carbon stocks between residential turf grass and native soil," *Urban Ecosyst.*, vol. 12, pp. 45–62, 2009.

[18] R. Lal, "Urban ecosystems and climate change," in *Carbon Sequestration in Urban Ecosystems*, R. Lal and B. Augustin, Eds. New York, NY, USA: Springer, 2012, pp. 3–19.

[19] A. Jacquin, L. Misakova, and M. Gaya, "A hybrid object-based classification approach for mapping urban sprawl in periurban environment," *Landscape Urban Plann.*, vol. 84, pp. 152–165, 2008.

[20] I. Vasenev, N. D. Ananyeva, and O. A. Makarov, "Specific features of the ecological functioning of urban soils in Moscow and Moscow oblast," *Eurasian Soil Sci.*, vol. 45, pp. 194–205, 2012.

[21] Å. Rosenqvist, A. Milne, R. Lucas, M. Imhoff, and C. Dobson, "A review of remote sensing technology in support of the Kyoto Protocol," *Environ. Sci. Policy*, vol. 6, pp. 441–455, 2003.

[22] J. M. Soriano-Disla, L. J. Janik, R. A. Viscarra Rossel, L. M. MacDonald, and M. J. McLaughlin, "The performance of visible, near-, and mid-infrared reflectance spectroscopy for prediction of soil physical, chemical, and biological properties," *Appl. Spectrosc. Rev.*, vol. 49, pp. 139–186, 2013.

[23] C. H. Wilcox, B. E. Frazier, and S. T. Ball, "Relationship between soil organic carbon and Landsat TM data in Eastern Washington," *Photogramm. Eng. Remote Sens.*, vol. 60, pp. 777–781, 1994.

[24] A. Stevens, B. Van Wesemael, G. Vandenschrick, S. Touré, and B. Tychon, "Detection of carbon stock change in agricultural soils using spectroscopic techniques," *Soil Sci. Soc. Amer. J.*, vol. 70, pp. 844–850, 2006.

[25] C. Gomez, R. A. Viscarra Rossel, and A. B. McBratney, "Soil organic carbon prediction by hyperspectral remote sensing and field vis-NIR spectroscopy: An Australian case study," *Geoderma*, vol. 146, pp. 403–411, 2008.

[26] J. F. Mas, "Monitoring land-cover changes: A comparison of change detection techniques," *Int. J. Remote Sens.*, vol. 20, pp. 139–152, 2011.

[27] P. Villa, "Mapping urban growth using soil and vegetation index and Landsat data: The Milan (Italy) city area case study," *Landscape Urban Plann.*, vol. 107, pp. 245–254, 2012.

[28] P. Villa, R. Scalenghe, and F. Malucelli, "Anthropogenic carbon stocks analysis in sparsely urbanized areas using remote sensing: A case study," in *Proc. Joint Urban Remote Sens. Event (JURSE)*, Apr. 21–23, 2003, pp. 119–122.

[29] R. Scalenghe *et al.*, "Influence of 150 years of land use on anthropogenic and natural carbon stocks in Emilia-Romagna Region (Italy)," *Environ. Sci. Technol.*, vol. 45, pp. 5112–5117, 2011.

[30] F. Ungaro, F. Staffilani, and P. Tarocco, "Assessing and mapping topsoil organic carbon stock at regional scale: A scorpan kriging approach conditional on soil map delineations and land use," *Land Degrad. Develop.*, vol. 21, pp. 565–581, 2010.

[31] Regione Emilia Romagna. (2011). *Uso del Suolo 2003edition 2011* [Online]. Available: http://geoportale.regione.emilia-romagna.it/it/catalogo/dati-cartografici/pianificazione-e-catasto/uso-del-suolo/2003-coperture-vettoriali-delluso-del-suolo-edizione-2011

[32] C. Song, C. E. Woodcock, K. C. Seto, M. P. Lenney, and S. A. Macomber, "Classification and change detection using Landsat TM data: When and how to correct atmospheric effects?," *Remote Sens. Environ.*, vol. 75, pp. 230–244, 2001.

[33] P. S. Chavez, Jr., "An improved dark-object subtraction technique for atmospheric scattering correction of multispectral data," *Remote Sens. Environ.*, vol. 24, pp. 459–479, 1988.

[34] P. Villa, "Imperviousness indexes performance evaluation for mapping urban areas using remote sensing data," in *Proc. Joint Urban Remote Sens. Event*, Paris, Apr. 11–13, 2007, pp. 1–6.

[35] P. Villa, M. Boschetti, F. Bianchini, and F. Cella, "A hybrid multi-step approach for urban area mapping in the Province of Milan, Italy," *Eur. J. Remote Sens.*, vol. 45, pp. 333–347, 2012.

[36] J. W. Rouse, R. H. Haas, J. A. Schell, and D. W. Deering, "Monitoring vegetation systems in the Great Plains with ERTS," in *Proc. 3rd ERTS Symp.*, Washington, DC, USA, NASA SP-351, 1973, pp. 309–317.

[37] M. Kawamura, S. Jayamana, and Y. Tsujiko, "Relation between social and environmental conditions in Colombo Sri Lanka and the Urban Index estimated by satellite remote sensing data," *Int. Arch. Photogramm. Remote Sens.*, Vienna, vol. 31, no. part B7, pp. 321–326, Jul. 12–18, 1996.

[38] Y. Shi, X. Sun, X. Zhu, Y. Li, and L. Mei, "Characterizing growth types and analyzing growth density distribution in response to urban growth patterns in peri-urban areas of Lianyungang City," *Landscape Urban Plann.*, vol. 105, pp. 425–433, 2012.

[39] J. Antle, S. Capalbo, S. Mooney, E. Elliott, and K. Paustian, "Spatial heterogeneity, contract design, and the efficiency of carbon sequestration policies for agriculture," *J. Environ. Econ. Manage.*, vol. 46, pp. 231–250, 2003.

[40] L. P. D'Acqui, A. Pucci, and L. J. Janik, "Soil properties prediction of western Mediterranean islands with similar climatic environments by means of mid-infrared diffuse reflectance spectroscopy," *Eur. J. Soil Sci.*, vol. 61, pp. 865–876, 2010.
[41] F. Saiano, G. Oddo, R. Scalenghe, T. La Mantia, and F. Ajmone-Marsan, "DRIFTS sensor: Soil carbon validation at large scale (Pantelleria, Italy)," *Sensors*, vol. 13, pp. 5603–561, 2013.

Paolo Villa received the Laurea (M.S.) degree in environmental engineering and the Ph.D. degree in geomatics from Polytechnic University of Milan, Milano, Italy, in 2004 and 2008, respectively.

He worked with the Remote Sensing Laboratory, Polytechnic University of Milan and the National Research Council of Italy, in CNR-ISTI and CNR-IREA institutes, where he is a Permanent Researcher since 2012. His work is framed into heterogeneous application fields ranging from land cover mapping and its change, geological mapping, agricultural crop identification, inland water basin assessment, urban area assessment, and natural hazards monitoring. His research interests include spatial data management, especially focusing on maritime and marine applications of SDI technologies, and digital multihyperspectral image processing, aimed at environmental phenomena mapping using Earth Observation.

Francesco Malucelli received the Laurea (M.S.) degree in geology and the Ph.D. degree in earth science from Alma Mater Studiorum, University of Bologna, Bologna, Italy, in 1991 and 1996, respectively.

He serves as an Executive Officer in the Servizio Geologico Sismico e dei Suoli—Regione Emilia-Romagna (Geological, Seismic and Soil Survey—Regione Emilia-Romagna, Italy), where he is working as a Pedologist. He is involved in different international and national projects dealing with soil science. His research interests include soils and land planning, soil ecosystemic function balance, soil carbon sink, soil awareness, soil micromorphology, and paleopedology.

Riccardo Scalenghe received the Laurea (M.S.) degree in agricultural sciences from the University of Torino, Torino, Italy, in 1989 and received the Ph.D. degree in soil chemistry from the University of Pisa, Pisa, Italy, in 1997.

In 1997, he lectured in soil science topics and later joined the Università degli Studi in Palermo, Palermo, Italy, in 2000, where he is conducting researches mainly on the human impact on soil environment.